Digest Journal of Nanomaterials and Biostructures Vol. 11, No. 4, October-December 2016, p. 1277-1288

PREPARATION AND CHARACTERIZATION OF NOVEL GELATIN/SILICA NANO-HYBRID AS A STYPTIC FOR MASSIVE BLEEDING

M. CHENANI[a], A. BEHNAMGHADER[b*], M. KHORASANI[c], M. AHMADINEJAD[d]

[a]*Biomaterials Group, Department of Medical Engineering, Science and Research Branch, Islamic Azad university, Tehran, Iran*

[b] *Biomaterials Group, Department of Nanotechnology and Advanced Materials, Materials & Energy Research Center, Karaj, Iran*

[c]*Department of Biomaterial, Iran Polymer and Petrochemical Institute (IPPI), P.O. Box: 14965, Tehran, Iran*

[d]*Iranian Blood Transfusion Organization Research Center, MD Pathologist, Tehran, Iran*

Effective hemorrhage control has become increasingly significant nowadays for civilian trauma, while currently available local haemostatic agents have been reported to have various drawbacks and side effects. In this study, a gelatin/silica nano-hybrid (GSNH) material has been designed to control massive bleeding. In particular, this nano-hybrid has been obtained from gelatin microspheres (GM) with nano-silica particles (NS), for hemorrhage control. Different concentrations of glutar-aldehyde (GA), from 0 up to 6 mol, were added to GM at certain ratio gelatin/silica, to achieve the optimum nano-hybrid. The thermal properties (Differential Scanning Calorimetry), chemical bonding and microstructure (Fourier Transform Infra Red), morphology (Field Emission Scanning Electron Microscopy), poly-dispersity index (Gel Permeation Chromatography), characterizes blood coagulation (Activated Partial Thromboplastin Time), blood and water absorption, as well as platelet adhesion (Lactate Dehydrogenase) properties of the novel GSNH have been investigated in order to assess the influence of GA concentration on the properties. The X-Ray Diffraction powder pattern confirms the amorphous nature of NS. These analyses have achieved extraordinary results demonstrating that the optimum nano-hybrid with GSNH-3GA formulation could significantly stanch blood induced platelet adherence, while maintaining its network structural integrity. Based on these results, it can be concluded that the GSNH developed here could be a promising candidate for stanch blooding control, valves hopefully raising chances of survival in severe bleeding.

(Received August 3, 2016; Accepted November 28,2016)

Keywords: Nano-Hybrid, Nano-Silica, Gelatin, Hemorrhage Control, Glutar-aldehyde

1. Introduction

Hybrid materials are designed with highly tailorable properties, which are achieved through careful control of synthesis parameters. These materials have great potential for biotechnological, biomedical and pharmaceutical applications, particularly as materials of high degree of compatibility with biological materials and as matrices for encapsulation of bioactive substances [1–2]. The design of metal oxide/polymer hybrid systems has attracted much attention in the last few years, due to their wide range of applications. Biopolymer/silica hybrid materials are composites inspired by nature, that permit to obtain a high compatibility with tissues and systems of biological origin [3–4]. According to the literature, gelatin/silica hybrids can find applications in bone regeneration strategies, angiogenesis, drug delivery and cements production [5–6], as well as in optical coatings, high refractive index films, contact lenses, thin film

*Corresponding author: a-behnamghader@merc.ac.ir

transistors, light emitting diodes, solar cells, optical waveguide materials and photo-chromic materials, for adsorption, catalysis and high energy fields [7–8–3].

Even though the properties of gelatin in aqueous solutions and in the gel state have already been extensively studied [9–10–12], a survey of the most recent literature clearly demonstrates that they still attract a great deal of attention[11–13–14]. Such an interest partly motivated by the range of application of gelatin colloids and matrices in the photographic processes [15–16], food industry and pharmaceutical delivery systems [17–18].

Apart from intrinsic properties (chain length and amino acid composition) and gelatin conditions (pH, temperature), the properties of gelatin gels can be modified by cross-linking agents, improving their thermal stability and mechanical properties [19–20–21].

Chemical cross-linking relies on gelatin chain bridging, via covalent bonding between the cross-linker and the amino groups of the protein [22–23–24]. Alternatively, hydrogen bonding properties of polyols can be used to induce physical cross-linking [25–26].

In this context, silica species can be considered as potentially interesting cross-linking agents since they were shown to interact through both electrostatic interactions and hydrogen bonding with some poly-amino acids and proteins [27–28]. Moreover, they can undergo condensation reactions leading to silica nanoparticles, films or continuous gel networks [20]. In the case of hybrid materials, of great importance is the formation of durable bonds between biopolymer and inorganic material. The essential role in the formation of such bonds is played silane coupling agents such as amino and epoxy functional silanes, etc. [8–29].

In this paper, we have presented syntheses of hybrid materials aimed at obtaining the highest ability to stanch the severe bleeding, which was achieved by integrating two types of materials: organic biopolymer (GM) and inorganic material (NS). Gelatin is a heterogeneous mixture of water-soluble proteins of a high molecular weight obtained from collagen, while its water solution readily forms gels at temperatures under 30℃.

It was expected that the amino acid residues contained in its protein structure could make possible an association with silica. This connectivity would allow good compatibility between both components leading to the formation of a hybrid composite. It should be mentioned that recently, gelatin/silica nano-hybrid has been prepared with potential application as a homeostatic materials for control of massive hemorrhage.

Nano-hybrid material was characterized by Differential Scanning Calorimetry (DSC), Gel Permeation Chromatography (GPC), Field Emission Scanning Electron Microscopy (FESEM), Fourier Transform Infra Red (FTIR), Activated Partial Thromboplastin Time (APTT), Lactate Dehydrogenase (LDH) assay as well as blood and water absorption experiments. The amorphous nature of NS confirms by X-Ray Diffraction (XRD) powder pattern. The results provide a basis for further development of stanch blood hybrids and, valves hopefully raising chances of survival in severe bleeding.

2. Materials and method

2.1. Materials

All the reagents used in this research such as gelatin type B from bovine skin, tetraethyl orthosilicate, calcium nitrate tetrahydrate, nitric acid 65% and acetone were purchased from Merck KGaA., Germany, and used as received without any further purification. All the other chemicals were of analytical reagent grade.

2.2. Preparation of GSNH

The nano-silica material was prepared by a Sol-Gel method, in which tetraethyl orthosilicate, calcium nitrate and nitric acid were its precursors[30].

To Obtain GM, gelatin was first heated to 60℃ in a bidistilled water, then emulsified with 250 ml olive oil to form a w/o emulsion in the presence of span 80. The emulsion was cooled to 4℃ and GA (25%) was used as a cross-linker. Samples cross linked at different concentrations of GA from 0 to 6 mol. After the cross-linking for 1hour, acetone was added to remove the oil, and microspheres were washed in water followed by acetone for several times and dried in air.

NS (0.12 gram) was separately stirred in bidistilled water (10 ml) for 1hour then GM (0.5 gram) was dissolved in that aqueous and stirred for 15 minutes till a homogenous colloid was obtained. Finally the nano-hybrid of gelatin/silica was obtained after frizz drying.

2.3. Characterization

The as-prepared SiO_2 powders were analyzed by XRD (X'Pert PRO MPD, Netherlands). This instrument works with voltage and current settings of 40 kV and 40 mA, respectively. For qualitative analysis, XRD diagram was recorded in the interval $10° \leq 2\theta \leq 80°$. DSC (Diamond DSC, United States) was performed at heating rate of $10^{℃}/_{min}$ with N_2 from 30℃ to 240℃ to evaluate the thermal stability and analyze the glass transition temperature (T_g) of nano-hybrid. Samples were placed in a hermetically encapsulated aluminum pan on a heating block, housed in DSC cell mounted in a calorimeter.

The recording of the infrared spectra was performed using a FTIR spectrometer (Shimadzu, Japan) from 400 cm^{-1} to 4000 cm^{-1} by the KBr pellet technique. FTIR was used to estimate the conformational change of the structure in GSNH nano-hybrid, cross-linked by GA. Additionally initial gelatin and prepared NS were characterized by FTIR. The nano-hybrid and NS morphology was observed with FESEM (VEGA/TESCAN, German) with an accelerating voltage of 3 kv, after being gold-coated. The FESEM images of NS was prepared by Sol-Gel in this study is shown in Figure 1a.

Each sample (1 mg) was placed in silicon tube containing HPLC grade water (1 ml) centrifuged for 30 min with a rotation rate 7000 rpm. Gel permeation chromatography (GPC, Agilent 1260) was used to determine supernatant weight-averaged molecular weight and poly-dispersity index (PDI) using water as the eluent and narrow poly-dispersity polyethylene glycol as the standards.

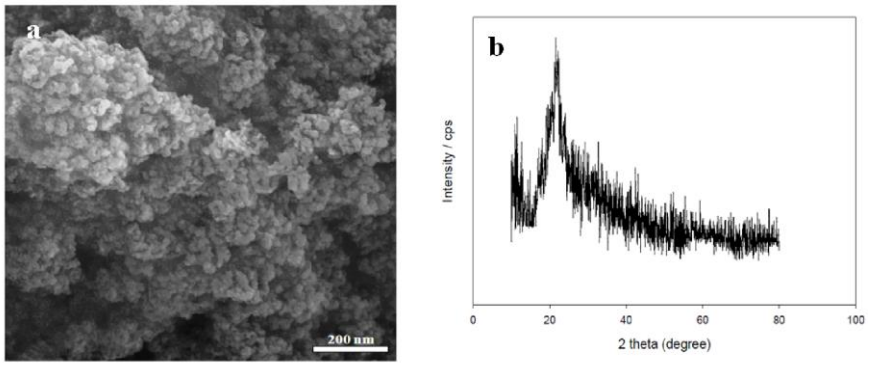

Fig. 1. FESEM image and XRD powder pattern of NS was prepared by Sol-Gel in this study.

2.4. Blood and water absorption

The absorption efficiency of materials was determined in whole blood and water by measuring the maximum amount of fluid absorption per unit weight of materials [31]. All samples were weighted and recorded for the initial weight (W_0), then immersed into blood. The weight of the samples was monitored until a constant value was reached (W_S). The blood absorption (S_W) was calculated as follows (Eq (1)).

$$\%S_W = \frac{Ws - W0}{W0} \times 100 \quad (1)$$

Water absorption was measured in exactly the same process by bidistilled water. Standard gauze was used as control.

2.5. Evaluation of the effect on the plasmatic phase of coagulation

The effect of the nano-hybrid on plasma coagulation activity was tested using activated partial thromboplastin time (APTT) test, which was performed using a semi-automatic coagulometer (Diagnostigua Stago, France). The study was approved by the Iranian Blood Transfusion Organization, the Coagulation Center. The platelet-poor plasma (PPP) was obtained by centrifugation at 3000 rpm for 15 minutes at 37℃. For APTT determination, various concentrations (0.01, 10 and 100 µg/mL) of GSNH-plasma complexes were incubated at 37℃ for 60 seconds [32].

2.6. Platelet adhesion

Platelet adhesion was determined using a LDH assay as described previously [33–34]. Human blood obtained from Iranian Blood Transfusion Organization, Tehran, in siliconized tubes containing 3.8% sodium citrate at a blood/citrate ratio of 9:1 and platelet rich plasma (PRP) was obtained by centrifugation at 150 gram for 15 minutes. Samples were incubated at 37℃ for 15 and 30 minutes in PRP with a number of platelets adjusted up to 425×10^3 μl^{-1}. Then non-adherent platelet were removed by washing 20 times with PBS. Thereafter the samples were placed into a 24 well plate, and the adhered platelets were lysates using LDH kit (Pars Azmoon, Iran). Clean gauze was used as a control. For each experimental condition, one set of samples (n=5) was used for platelet adhesion measurements. UV absorption were studied at a wavelength of 340 nm.

3. Results and Discussion

3.1. XRD analysis

The strong and broad XRD pattern at $2\theta = 22°$ of NS (Figure 1b) shows the prepared NS is amorphous, which is crucial to achieve a super hydrophilic nano-hybrid [35]. Functional groups of an intrinsic NS surface consist of silanol (Si-OH) and siloxane (Si-O-Si) groups. Increasing the number of silanol groups leads to increasing hydrophilicity and water absorption of NS. In fact, for water absorption of NS, the main role is played by free hydroxyl groups and siloxane bridge. The concentration of surface hydroxyls on amorphous silica is about 5 hydroxyl groups per nm^2, which corresponds to one hydroxyl per silicon atom, thus water is strongly adsorbed on the amorphous NS surface.

3.2. DSC analysis

The DSC curve for all samples (Figure 2) showed characteristic endothermic transitions of structural changes of the material related to the energy during process. It was found from DSC curve that the nano-hybrid structure changed due to the protein denaturation at 30 ℃-240 ℃.

There are two significant events that appear on the DSC graph:

I. T_g slowly increases with increasing amounts of GA.

II. Heat flow changes is also reduced by reducing the amount of GA.

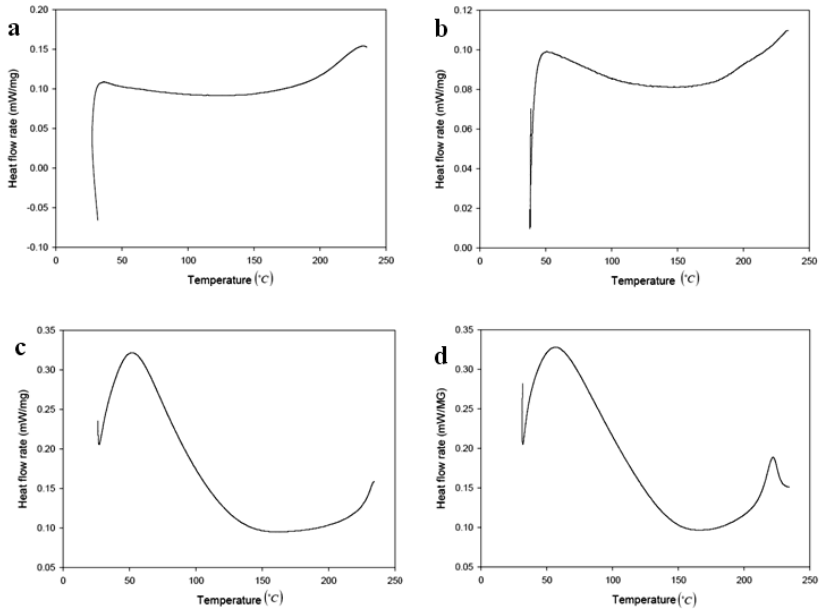

Fig. 2. DSC curve of GSNH-0GA (a), GSNH-1GA (b), GSNH-3GA (c) and GSNH-6GA (d).

In fact, when GA isn't in the nano-hybrid structure, the NS intermolecular interaction with GM (polar interaction of COOH of GM with Ca^{2+} in NS and/or hydrogen interaction of NH_2 of GM with SiOH of NS), shows that GM is more inclined to the fourth structure (or Triple Helix). It is generally accepted that the endothermic process present in the DSC thermo-gram of gelatin material involves rupture of hydrogen bonds and a rearrangement of the Triple Helix into a random configuration [36–37].

So when GM maintain the structural integrity of Triple Helix in the sample, thermal denaturation occurs at the specific time, without any heat transfer at the temperatures applied, and with a minimum of enthalpy changes [38–39]. However, with increasing amounts of GA Alpha Helices and Beta Sheet chains retain their structure. And it is known that the thermal helix-coil transition depends on the degree of hydration [40]. Furthermore, it was previously shown that the more gelatin materials are cross linked, the less they can bind water [41–42-43]. In fact, cross-linked GA inhibits the movement of gelatin chains, and the presence of NS that is placed on the exterior gelatin, increases T_g and samples thermal stability.

ΔH is the amount of heat energy required to bring about the transition. An increase in ΔH indicates that cross linking has occurred, which then requires more energy to undergo the helix-coil transition. The ΔH results of all samples declared in table 1 separately. It could be observed that the GSNH-6GA exhibits a marked increase in the denaturation peak temperature as well as in the enthalpy changes when compared to GSNH-0GA. Similar observations were reported in previous study [44–45].

Table 1. Enthalpy changes (ΔH) results of GSNH with different concentrations of GA from 0 up to 6 mol.

	GSNH-0GA	GSNH-1GA	GSNH-3GA	GSNH-6GA
$\Delta \boldsymbol{H}\ \left(^{\boldsymbol{J}}/_{\boldsymbol{g}}\right)$	17.36	21.78	34.53	37.15

3.3. GPC analysis

Some important results were obtained through GPC analysis, as listed in Table 2. For all samples, PDI was close to 1 that means gelatin reached its optimum conditions in the ultimate nano-hybrid [46]. This PDI indicates that the free amino groups on gelatin react with GA, leading

to formation of a network structure that limits the mobility of the polymer chains, aggravated further by increasing GA.

Increasing the amount of GA leads to decreasing number and length of chain which have come into the supernatant. This confirms increasing amount of cross-linked gelatin and terminating higher stability in nano-hybrid.

Table 2. The number average molecular weight (M_n), the weight average molecular weight (M_w) and PDI of samples

	GSNH-0GA	GSNH-1GA	GSNH-3GA	GSNH-6GA
M_n(g/mol)	2.88×10^4	2.39×10^4	9.51×10^3	3.05×10^3
M_w(g/mol)	3.17×10^4	2.54×10^4	1.46×10^4	3.11×10^3
PDI	1.10	1.06	1.54	1.02

3.4. FTIR analysis

The FTIR spectrum of the nano-hybrid is shown in Figure 4. When compared with Figure 3a (NS) and 3b (gelatin), the impact of hybridization is evident, with details discussed in the following. The spectrum of Figure 3a exhibits a number of characteristic spectral bands [47]. The peaks at 1110 cm^{-1} and 800 cm^{-1} are due to Si-O-Si bending modes, including symmetric Si-O-Si stretching vibration and asymmetric Si-O-Si stretching vibration, respectively. These are specific bands of NS. The peak at 968 cm^{-1} is ascribed to the stretching vibration of Si-OH. The absorption bands at 3600 cm^{-1} and 1656 cm^{-1} are assigned to the H-O-H stretching and bending modes of the adsorbed water, respectively, related to the silanol -OH groups and water bound to the silica surface.

The characteristic spectral bands of gelatin are visible in Figure 3b. The sharp and broad peak at 1600-2100 cm^{-1} indicates amid I. Amid I band is mainly due to C=O stretching vibration of the amid group coupled with in-plane N-H band [48-49]. Amid II is driven mainly by in-plane N-H at 1417 cm^{-1}. In addition, amid III and amid A bands were detected at 993 cm^{-1} and 3555 cm^{-1}, respectively.

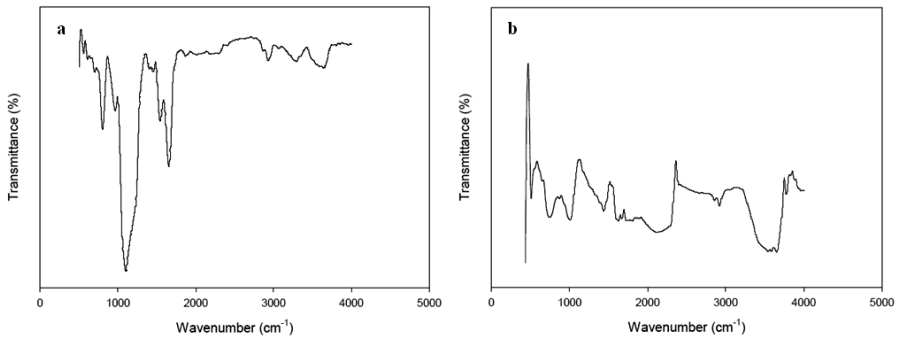

Fig. 3. FTIR spectra of NS (a) and gelatin (b).

As is clear, the slight change in the shapes of samples peaks occurred after adding NS to GM. It is generally acknowledged that NS and GA have competitive effects on the nano-hybrid structure, which is well reflected in the FTIR spectrum. The distributions of hydrophilic and hydrophobic surfaces, as well as positive and negative charges of the side chains of protein structure, have a major impact on the processes of adsorption. In this study, the NS has a direct effect on the ultimate structure of the nano-hybrid which has no GA (GSNH-0GA, Figure 4) and strongly affects the hydrophilic behavior of the nano-hybrid.

In fact, the wave location of amid A for GSNH-0GA (3424 cm^{-1}) was lower than that for GSNH-6GA (3595 cm^{-1}), with still a lower location of amid I (1737 cm^{-1}) and amid II (1452 cm^{-1}) peaks.

However, a wide and higher amid III (1162 cm^{-1}) peak could be observed. During the hybridization of GSNH-0GA, the Ca^{2+} ions (which are in the NS structure) make a covalent band with RCOOH of GM molecules. Moreover, the cross-linking induces the shortening of the distance between GM chains within the critical length, so triple-helix will have a more chance to become manifest.

But the nano-hybrid cross-linked by GA showed an increase in adsorption band intensity for amid A, indicating that most of the NS was trapped by the GM which is confirmed by the SEM results. In the GSNH-6GA, β-sheet augmentation slightly reshaped amid I peak, which indicates that GSNH-6GA adopts a predominantly α-helix and β-sheet configuration [50].

Lower frequencies of amid I bands can be attributed to a certain dominance of the molecular order of triple-helix. The H-bonded network at the N-H side shows a decrease in electronic density, resulting in a decrease in negative charges of oxygen and nitrogen. The decrease in H-bonding at N-H shortens the N-H and C=O bond length, decreasing the amid II vibration band frequency. However, the contribution of H-bonding and C=O to the amid II band is relatively small.

Additionally, the position of the band in amid A region shifts to lower frequencies, indicating the involvement of the N-H group of shorter peptide fragments in hydrogen bonding. The shifts of amid I band (from 1757 cm^{-1} to 1737 cm^{-1}) and amid II band (from 1571 cm^{-1} to 1452 cm^{-1}) substantiate changes in H-bonding density at N-H and C=O sites. The water and blood absorption results approved these effects exactly.

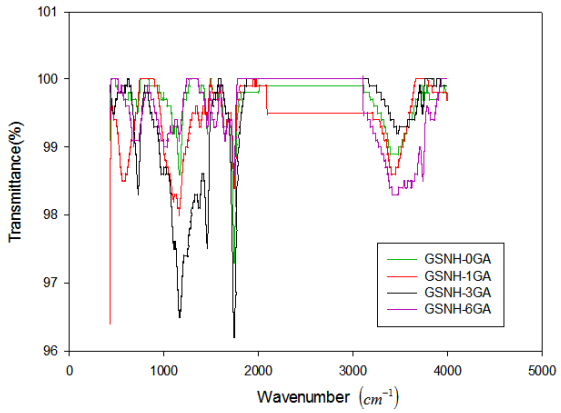

Fig. 4. FTIR spectra of nano-hybrid (GSNH-6GA, GSNH-3GA, GSNH-1GA and GSNH-0GA).

3.5. FESEM observation

The FESEM images of GSNH (Figure 5) reveal that at any GA concentration, GM can be observed significantly throughout the nano-hybrid except for the GSNH-0GA that is free of GA (Figure 5a). In general, this result clearly indicate that there is a difference in the surface morphology and mean particle size between GSNH-1GA, GSNH-3GA and GSNH-6GA. In this study reveal that GSNH-6GA has a rough surface (Figure 5d) compare to the smooth and flat morphology of GSNH-1GA, which is consist with the result of previous studies [51–52-53]. In this imposition, the positively charged GM could adsorb and concentrated the negatively charged NS via electrostatic and hydrogen bond interactions, with increasing NS concentration around the outer surface of GM beads. The silicon atoms were brought into close proximity and the condensation process occurred afterwards by forming Si-O-Si bonds.

The typical FESEM images in Figure 5b and 5c shows the diameters of the GSNH-1GA and GSNH-3GA were approximately 75 µm and 22 µm respectively. As can be seen, with raising GA concentration about 6 mol, the surface of the nano-hybrid became rough with wrinkles that spherical nano-hybrid about 12 µm in diameter. Because of more and more NS built-up around the outer surface of the GM beads, and aggregation with other adjacent precursors through the condensation reaction between the surface silanol groups, this process ultimately results in the formation of an intact silica shell. As shown in Figure 5c, optimum nano-hybrid beads were fairly

rough and wrinkles, as compared with the surface of GSNH-1GA. Appearance of the microspheres surface and their mean particle size should be attributed to the fact that amount of the cross-linking agent influence the size and morphology of GA cross linked nano-hybrid.

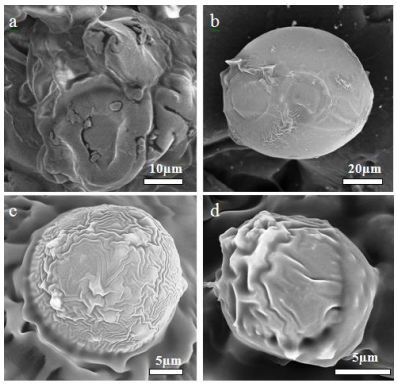

Fig. 5. FESEM images of GSNH-0GA (a), GSNH-1GA (b), GSNH-3GA (c), GSNH-6GA (d).

3.6. Blood and water adsorption

The blood and water absorption of the GSNH with various GA concentration are presented in Figure 6. The blood absorption ratio was about 196.4% of weight of GSNH-0GA samples where as 302.5% of weight of GSNH-1GA, 435.8% of weight of GSNH-3GA and 246.2% of weight of GSNH-6GA. This value for water was about 153.2%, 294.8%, 380.3% and 201.3% respectively. It is clear that the fluid absorption ratio did not differ significantly between the blood and water for either amount of GA of 0, 1 and 6 mol but was significantly higher for 3 mol (380.3% and 435.8%) than in GSNH-0GA, GSNH-1GA, GSNH-6GA and gauze (204.1% and 206.8%), which suggested that the GSNH-3GA had higher absorption capacity. Because of with increasing the concentration of GA up to 3 mol, NS was placed within the gelatin structure due to electrostatic reactions. So MG with a greater number of functional hydroxyl group R-OH absorbed higher rates of blood and water. However, the most gelatin N terminal involved with Si-OH was trapped within the chains.

It is clearly evident from Figure 6 that by increasing the amount of GA about 6 mol, most NH terminal amino acids has blocked and the presence of NS in the form of silanol groups Si-OH reacted with remaining amino acids for the following two reasons, severely reducing blood and water adsorption.

1. Cross-linked gelatin increases, so any absorbed water is due to the pores in cross-linked spaces.
2. Non-polar NS bonds such as Si-OH react with gelatin, and are exposed to interactions with the environment and the hydrophobic siloxane placed on the surface of NS.

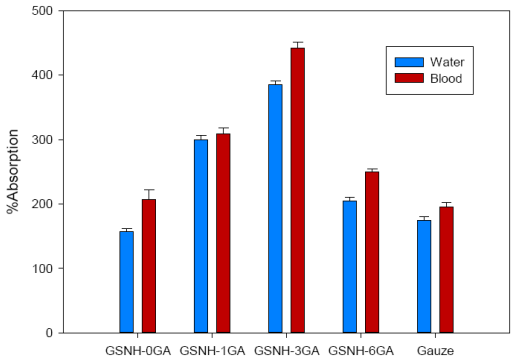

Fig. 6. Blood and water adsorption ratio for GSNH with different concentrations of GA from 0 up to 6 mol and gauze

3.7.APTT test

A critical component of the blood coagulation cascade is fibrinogen. It is the most abundant protein in the elution from the colloidal surfaces. Blood coagulation involves a series of proteolytic reactions resulting in the formation of fibrin clot. Thrombin is formed following a cascade reaction where an inactive factor becomes enzymatically active after proteolytic cleavage by other enzymes and the newly activated enzyme then activates another inactive precursor factor [54–55].

The APTT test is used to check the internal coagulation pathway, which is one of the standard medical tests. APTT is measured inside the clot formation pathway from the beginning of the process to the final stage. The internal pathway has a much slower progress and usually requires one to six minutes to create clots [56]. Here, we have examined the interaction of the plasma fibrinogen with the GSNH, NS, GM and studied their influence on blood coagulation using APTT.

Formation of a fibrin clot in plasma requires a few seconds after the addition of the partial thromboplastin reagent and calcium chloride to the samples. APTT results of plasma (control), NS, GM, nano-hybrid (GSNH-0GA, GSNH-1GA, GSNH-3GA and GSNH-6GA) plasma complexes are shown in figure 8. The control APTT time for a healthy blood plasma was measured to be about 31.2 seconds. When the blood plasma was incubated with GM, NS and nano-hybrid with various concentrations of GA, the corresponding data of APTT were 29.8 seconds (GM) and 30.5 seconds (NS) for 0.01 µg/mL, 28.6 seconds (GM) and 28.9 seconds (NS) for 10 µg/mL, and 27.4 seconds (GM) and 25.1 seconds (NS) for 100 µg/mL, respectively. It can be seen that APTT was significantly shortened by GM and NS compared with the control (plasma = 31.2 seconds).

Surprisingly, in the APTT results of the nano-hybrid, no significant difference was observed in the presence or absence of GA with various concentrations in blood plasma. In fact, in all GSNH nano-hybrid samples, clots were formed before adding reagent and it was not possible to perform the APTT test in the presence of GSNH. Creating a hybrid of NS and GM reduces coagulation time which can not be measured, due to water absorption of GSNH nano-hybrid.

Generally, hydrophilic/hydrophobic surfaces play an important role in the absorption of proteins on the surface. Studies have shown that plasma coagulation on the hydrophilic surface is much more efficient compared with the hydrophobic surface [57-58]. The hydrophilic surfaces are categorized into anionic and cationic groups, based on their surface charge. The anionic surfaces are stronger than the cationic surfaces, in terms of the plasma coagulation. So the most effective method for plasma coagulation is the application of an active anionic hydrophilic material, such as GSNH nano-hybrid.

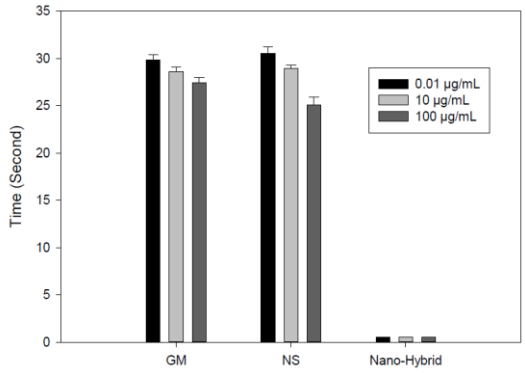

Fig. 7. APTT clotting test for interaction of plasma with GM, NS and nano-hybrid (GSNH with different GA from zero to 6 mol).

3.8. Platelet adhesion

Platelet adhesion was qualitatively determined by a modified lactate dehydrogenize (LDH) method and the results are presented here as the UV absorption (Figure 8). It can be seen that

compared with the control, the platelets adhered to all of the samples significantly increased, as the number of platelets adhered to the surface increased with increasing GA.

In GSNH-6GA, the amount of platelets adhering to the surface is more than other cases during the initial time, but the difference between the samples over the time span of 30 minute is a little less, so that the GSNH-3GA shows the highest platelets adhesion after 30 minutes. As soon as the nano-hybrid is exposed to blood, its humidity wets the nano-hybrid as a first stage and then proteins are absorbed to it. When applied onto the blood, the GSNH agents sequester a large amount of water (more than 435.8% by weight as shown in blood and water as adsorption test) and concentrate the cellular and plasma components in the haemorrhaging blood, and this will assist in primary hemostasis by physically forcing the platelets and accelerate the turnover of coagulation cascade for thrombin generation and thus help forming blood clots.

Another crucial parameter affecting the hemostatic activity of GSNH might be attributed to the calcium ions that released from material into blood. It is well established that, the calcium ions can help induce the activation and turnover of the intrinsic coagulation cascade with other clothing factors and thus accelerate the production of sufficient amounts of thrombin to support earlier fibrin generation [59].

Due to Vorman effect and the fact that albumin is most absorbed in tyrosine, it was proved that increasing the amount of GA leads to albumin showing more resistance against succession on the surface of nano-hybrid, hence attraction of more platelets on the surface.

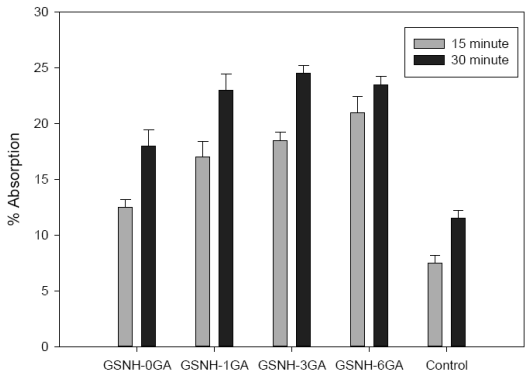

Fig. 8. Platelet adhesion to the GSNH materials after different incubation time in PRP by UV absorption

4. Conclusions

In the present study, an ordered GM with different amounts of GA hybridization with NS, has been developed for hemorrhage control and its haemostatic efficacy together with the protection nano-hybrid network has been evaluated.

In GSNH-3GA (the optimal nano-hybrid),T_g and thermal stability are at their optimum level, because the Alpha Helix and Beta Sheet structure conformations are at their highest, and the presence of NS causes more accumulation on the surface of the GM in the nano-hybrid.

Blood absorption was observed when NS was placed within the gelatin structure, through electrostatic reactions. Gelatin with a greater number of hydroxyl functional groups R-OH absorbed higher rate of blood, as confirmed with LDH analyses.

A good agreement between Blood and water absorption, FESEM images and LDH analyses with DSC, proved that GSNH-3GA is the best to recommend for stanch blooding control. We believe this study demonstrates the haemostatic property of nano-hybrid materials. Further studies are required to clarify the mechanism of their haemostatic activity.

Acknowledgments

The authors would like to thank Iranian Blood Transfusion Organization Coagulation Center that has made a vast contribution to this research.

References

[1] P. Judeinstein, C. Sanchez. J. Mater. Chem. **6**, 511 (1996).
[2] G.L. Yuan, M.Y. Yin, T.T. Jiang, et al. Catal. A: Chem., **159**, 45 (2000).
[3] I. Brasack, H. Bottcher, U. Hempel. Sci. J. Technol. 19, 479 (2000)
[4] L. Ren, K. Tsuru, S. Hayakawa. Biomaterials.; **23**, 4765 (2002).
[5] M. Schuleit, P.L. Luisi. Biotechnol. Bioeng.; **72**, 249 (2001).
[6] M.R. Ayers, A.J. Hunt. J. Non-Cryst. Solids. **290,** 122 (2001)
[7] M. Menning, K. Fries, M. Lindenstruth, et al. Thin Solid Films. **351,** 180 (1999)
[8] T.P. Chou, C. Chandrasekaran, S.J. Limmer, et al. J. Non-Cryst. Solids. **290**, 153 (2001)
[9] A.J. Kuijpers, G.H. Engbers, J. Feijen, et al. Macromolecules. **32**, 249 (1999).
[10] M.Djabourov, J.Leblond, P.Papon. Structural investigation. de Physique. **49**, 319 (1988)
[11] P.J. Flory, R.R. Garrett. J. Am. Chem. Soc. **80,** 4836 (1958)
[12] K. te Nijenhuis, Adv. Thermoreversible Networks. 130th ed. Springer: Polym. Sci., 1997, p. 170.
[13] V. Normand, A. Parker. Soft Matter. **6**, 4916 (2010).
[14] C. Joly-Duhamel, D. Hellio, M. Djabourov. Langmuir. **18**, 7208 (2002);
[15] T. H. James. The theory of the photographic process. 4th ed. New York: Macmillan, 1977, p.128.
[16] A.M. Howe, C. Opin. Some aspects of colloids in photography . Colloid Interface Sci.; **5**, 288 (2000).
[17] E. Dickinson, D.T. Wasan, Colloid Interface Sci. **1**, 709 (1996).
[18] J. J. Marty, R. C. Oppenheim, P. Speiser,. Pharm. Acta Helv. **53**, 17 (1978).
[19] T. Coradin, A. Coupe, J. Livage Colloids Surf. B. **29,** 189 (2003).
[20] R.K. Iler, The Chemistry of Silica: Solubility, Polymerization, Colloid and Surfaces Properties, and Biochemistry.1th ed. New York: Wiley, 1979, p.763.
[21] M. Fujitsu, M. Hattori, T. Tamura. Colloid Polym. Sci. **275**, 67 (1997).
[22] J. Sharma, H.B. Bohidar, Colloid Polym. Sci. **278**, 15 (2000).
[23] S.G. Clark, P.F. Holt, C.W. Went. Trans. Faraday Soc. **53**, 1500 (1957).
[24] T. Abete, E. D. Gado, L. Arcangelis, Polym. Compos. **34**, 259 (2013).
[25] J. Wu, S.C. Chiu, E. Pearce, et al. J. Polym. Sci. A. **39**, 224 (2001).
[26] V.G Kadajji, G. V. Betageri. Polym. **3**, 1972 (2011).
[27] T. Coradin, J. Livage. Mater. Scien. Engin. C. **25**, 201 (2005).
[28] Q. Chen, F. Miyaji, T. Kokubo, et al. Biomaterials. **20**, 1127 (1999).
[29] T. Coradin, J. Allouche, M. Boissière, et al. Curr. Nanoscien. **2**, 1 (2006).
[30] A. Venkateswara, Sharad D.Bhagat. Solid State Sciences. **6**, 945 (2004).
[31] Ong SY, Wu J, Moochhala SM, et al. Biomater. **29**, 4323 (2008).
[32] J. Mona, C. J. Kuo, E. Perevedentseva, A. V. Priezzhev, et al. Diam. Rela. Mater. **39,** 73 (2013).
[33] JM. Grunkemeier, WB. Tsai, CD. Mcfarland, et al. Biomaterials. **21**, 2243 (2000).
[34] Vanickova M, Suttnar J, Dyr JE. Platelets. **17**, 470 (2006).
[35] P. Worathanakul, W. Payubnop, A. Muangpet. Wor. Aca. Scie. Engi. Tech. **56**, 360 (2009).
[36] D. Achet, XW He, Polym. **36**, 787 (1995).
[37] A. Tanioka, K. Miyasaka, K. Ishikawa. Biopolym. **15**, 1505 (1976).
[38] M. M. Horn, V. C. Martins, Carbohyd. Polym. **77**, 239 (2009).
[39] Yu. N. Sazanov, A. V. Gibanov, V. A. Lysenko. Fib. Chem. **40**, 355 (2008).
[40] NM. Pineri, M. Escoubes, G. Roche. Biopolym. **17**, 2799 (1978).
[41] AN. Fraga, RJJ. Williams. Thermal properties of gelatin films . Polym. **26**, 113 1985.
[42] J. Kopp, M. Bonnet. Matrix. **9**, 443 (1989).

[43] A. Bigi, M. Borghi, G. Cojazzi, et al. Thermal Anal. **61**, 451 (2000).
[44] J. H. Choi, J. Jegal, W.N. Kim, et al. Application Polymer Science. **111**, 2186 (2009).
[45] Q. Cheng, F. Pan, B. Chen, et al. Membr. Scien. **363,** 316 (2010).
[46] J. Martinez-Diaz, D. Nelson, C.Crone. Chem. Phys. **204**, 1898 (2003).
[47] M. Liu, L. Gan, L. Chen, D. Zhu, et al. Int. J. Pharm. **427**, 354 (2012).
[48] M. F. Butler, Y. F. Ng, Pudney, J. Poly. Scie. Part A poly. Chem. **41**, 3941 (2003);
[49] T. Elzein, M. Nasser-Eddin, C. Delaite et al. J. Colloid Interface Sci. **273**, 381 (2004)
[50] H. D. Wang, C.Hui Niu, Q.Yang, et al. Nanotechnology. **22**, 145703 (2011).
[51] M. Jabli, M.H.V. Baouab, N. Sintes-zydowicz, et al. [Dye molecules/copper (II)/macroporous glutaraldehyde-chitosan] microspheres complex: surface characterization, kinetic, and thermodynamic investigations . Appl. Polym. Sci. **123**, 3412 (2012).
[52] B.E. Mirzaei, S.A.A. Ramezani, M. Shafiee, et al. Polym. Mater. **62**, 605 (2013).
[53] E.L. Mcconnell, S. Murdan, A.W. Basit, et al. Pharm. Sci. **97**, 3820 (2008).
[54] D. Kim, H. El-Shall, D. Dennis, et al. Colloids Surf. B: Biointerfaces. **40**, 83 (2005).
[55] A. Radomski, P. Jurasz, D. Alonso-Escolano. Br. J. Pharmacol. **146**, 882 (2005).
[56] J. Semberova, S.H. De Paoli Lacerda. Nano Lett. **9**, 3312 (2009).
[57] T. Ikeda, Kuroda. Collo. Sur. B: Biointer. **86**, 359 (2011).
[58] M. Rabe, D. Verdes, S. Seeger. Adv. Coll. Inter. Scie. **162,** 87 (2011).
[59] B. Furie, B.C. Furie. Thrombus formation in vivo . Clin. Invest. **115**, 3355 (2005).